

Free Energy and Plaquette expectation value for gluons on the lattice, in three dimensions

H. Panagopoulos^a, A. Skouroupathis^a and A. Tsapalis^b

^a*Department of Physics, University of Cyprus, P.O. Box 20537, Nicosia CY-1678, Cyprus*
email: haris@ucy.ac.cy, php4as01@ucy.ac.cy

^b*University of Athens, Institute of Accelerating Systems and Applications, Athens, Greece*
email: a.tsapalis@iasa.gr

(November 5, 2018)

Abstract

We calculate the perturbative value of the Free Energy in Lattice QCD in three dimensions, up to three loops. Our calculation is performed using the Wilson formulation for gluons in $SU(N)$ gauge theories.

The Free Energy is directly related to the average plaquette. To carry out the calculation, we compute the coefficients involved in the perturbative expansion of the Free Energy up to three loops, using an automated set of procedures developed by us in Mathematica. The dependence on N is shown explicitly in our results.

For purposes of comparison, we also present the individual contributions from every diagram. These have been obtained by means of two independent calculations, in order to cross check our results.

Keywords: Lattice QCD, Lattice perturbation theory, Free Energy.

I. INTRODUCTION

In this paper we calculate the Free Energy of QCD on the lattice, up to three loops in perturbation theory. We are interested in the three dimensional case, involving only gluons.

The choice of studying the Free Energy is motivated by the fact that, apart from being a simple physical observable which can be calculated in perturbation theory, it is used to determine the static thermodynamic properties of a physical system. Furthermore, this quantity is ideal for studying various aspects of QCD. For example, the Free Energy is often employed in the context of thermal QCD, for the purpose of characterizing the deconfinement transition between the low temperature regime, ruled by confinement, and the high temperature regime ruled by asymptotic freedom. Asymptotic freedom guarantees a small coupling constant at large temperatures, which in turn allows for a perturbative evaluation of observables. In addition to that, the perturbation expansion of the Free Energy is involved in the determination of the “finite part” of the gluon condensate in lattice regularization.

Finally, the plaquette expectation value, which is directly related to the Free Energy, is considered in the study of an effective 3-D pure gauge theory called Magnetostatic QCD (MQCD) [1], which is matched to QCD using perturbation theory. Due to the superrenormalizable nature of the 3-D theory, only a finite number of divergences arise and these can be computed perturbatively, allowing for a complete match between the lattice regularization scheme and a continuum scheme such as \overline{MS} . MQCD is an instance of “dimensional reduction”, whereby the static properties of a (3+1)-dimensional field theory at high temperature can be expressed in terms of an effective field theory in 3 space dimensions. Dimensional reduction has been applied to QCD (see, e.g., [2,3]), in order to resolve a longstanding problem regarding the breakdown of the perturbation expansion for the Free Energy [4].

The evaluation of the Free Energy in four dimensions has already been carried out to 2 loops [5] and 3 loops [6,7]. In three dimensions, the only results available so far have been obtained through the method of stochastic perturbation theory [8]. Our results can be used both for comparison with existing results extracted from different methods, or for calculations involving the perturbative expansion of the Free Energy. With respect to this, the coefficients of the perturbative expansion allow the subtraction of all the divergent contributions from the gluon condensate [9] and improve the previous estimates of Ref. [8].

II. CALCULATION

In standard notation the Wilson action for gluons reads:

$$S_L = \frac{1}{g_0^2} \sum_{x, \mu, \nu} \text{Tr} [1 - U_{\mu, \nu}(x)] \quad (1)$$

Here $U_{\mu, \nu}(x)$ is the usual product of link variables $U_\mu(x)$ along the perimeter of a plaquette in the μ - ν directions, originating at x ; g_0 denotes the bare coupling constant. Powers of the lattice spacing a have been omitted and may be directly reinserted by dimensional counting.

We use the standard covariant gauge-fixing term [10]; in terms of the gauge field $Q_\mu(x)$ [$U_\mu(x) = \exp(i g_0 Q_\mu(x))$], it reads:

$$S_{gf} = \lambda_0 \sum_{x,\mu,\nu} \text{Tr} \{ \Delta_\mu^- Q_\mu(x) \Delta_\nu^- Q_\nu(x) \}, \quad \Delta_\mu^- Q_\nu(x) \equiv Q_\nu(x - \hat{\mu}) - Q_\nu(x). \quad (2)$$

Having to compute a gauge invariant quantity, we chose to work in the Feynman gauge, $\lambda_0 = 1$. Covariant gauge fixing produces the following action for the ghost fields ω and $\bar{\omega}$

$$\begin{aligned} S_{gh} = 2 \sum_{x,\mu} \text{Tr} \left\{ \left(\Delta_\mu^+ \omega(x) \right)^\dagger \left(\Delta_\mu^+ \omega(x) + i g_0 [Q_\mu(x), \omega(x)] + \frac{i g_0}{2} [Q_\mu(x), \Delta_\mu^+ \omega(x)] \right. \right. \\ \left. \left. - \frac{g_0^2}{12} [Q_\mu(x), [Q_\mu(x), \Delta_\mu^+ \omega(x)]] \right. \right. \\ \left. \left. - \frac{g_0^4}{720} [Q_\mu(x), [Q_\mu(x), [Q_\mu(x), [Q_\mu(x), \Delta_\mu^+ \omega(x)]]]] \right] + \dots \right\}, \\ \Delta_\mu^+ \omega(x) \equiv \omega(x + \hat{\mu}) - \omega(x). \end{aligned} \quad (3)$$

Finally the change of integration variables from links to vector fields yields a Jacobian that can be rewritten as the usual measure term S_m in the action:

$$S_m = \sum_{x,\mu} \left\{ \frac{N g_0^2}{12} \text{Tr} \{ (Q_\mu(x))^2 \} + \frac{N g_0^4}{1440} \text{Tr} \{ (Q_\mu(x))^4 \} + \frac{g_0^4}{480} \left(\text{Tr} \{ (Q_\mu(x))^2 \} \right)^2 + \dots \right\} \quad (4)$$

In S_{gh} and S_m we have written out only terms relevant to our computation. The full action is:

$$S = S_L + S_{gf} + S_{gh} + S_m. \quad (5)$$

In D-dimensions, the average value of the action density, S/V , is directly related to the average 1×1 plaquette P :

$$\langle S/V \rangle = \frac{D(D-1)}{2} \beta \langle E(P) \rangle. \quad (6)$$

where:

$$E(P) = 1 - \frac{1}{N} \text{Re}[\text{Tr}(P)], \quad \beta = \frac{2N}{g_0^2} \quad (7)$$

We will calculate $\langle E \rangle$ in perturbation theory:

$$\langle E \rangle = c_1 g_0^2 + c_2 g_0^4 + c_3 g_0^6 + \dots \quad (8)$$

The n -loop coefficients c_n have been known for some time up to 3 loops in the 4-dimensional theory [6].

The calculation of c_n proceeds most conveniently by computing first the Free Energy $-(\ln Z)/V$, where Z is the full partition function:

$$Z \equiv \int [\mathcal{D}U] \exp(-S). \quad (9)$$

The average of E is then extracted as follows:

$$\langle E \rangle = - \left(\frac{D(D-1)}{2} \right)^{-1} \frac{\partial}{\partial \beta} \left(\frac{\ln Z}{V} \right). \quad (10)$$

In particular, the perturbative expansion of $(\ln Z)/V$ is:

$$(\ln Z)/V = d_0 - \frac{(D-1)}{2} (N^2-1) \ln \beta + \frac{d_1}{\beta} + \frac{d_2}{\beta^2} + \dots \quad (11)$$

We can now write the perturbative expansion of $\langle E \rangle$, by combining Eqs. (10) and (11):

$$\langle E \rangle = \left(\frac{D(D-1)}{2} \right)^{-1} \left[\frac{(D-1)(N^2-1)}{2} + \frac{d_1}{\beta^2} + \frac{2d_2}{\beta^3} + \dots \right] \quad (12)$$

The coefficients c_n involved in Eq. (8) can be specified by the general expression

$$c_n = \left(\frac{D(D-1)}{2} \right)^{-1} \frac{(n-1)d_{n-1}}{(2N)^n}, \quad n \geq 2 \quad (13)$$

which leads immediately to the following relations for $D = 3$:

$$c_2 = d_1/(12N^2), \quad (14)$$

$$c_3 = d_2/(12N^3). \quad (15)$$

III. RESULTS

A Total of 36 Feynman diagrams contribute to the present calculation, up to three loops, as shown in Figure 1. The involved algebra of the lattice perturbation theory was carried out using our computer package in Mathematica. The value for each diagram is computed numerically for a sequence of finite lattice sizes L , followed by an extrapolation to $L \rightarrow \infty$ (see next Section). The finite- L results, on a per diagram basis, are available upon request from the authors. We performed two independent calculations for each diagram, in order to verify our results.

Certain diagrams, considered individually, are infrared divergent; they contain subdiagrams which renormalize the gluon propagator to one loop, as shown in Figure 2. Taken as a group, these diagrams become infrared finite and their value can be extrapolated to infinite lattice size; extrapolation leads to a (small) systematic error, which is estimated quite accurately.

The coefficients c_i involved in the perturbative expansion of $\langle E \rangle$ can be calculated by summing all contributing diagrams. They take the form:

$$\begin{aligned} c_1 &= \frac{N^2-1}{6N}, \\ c_2 &= \sum_j \frac{(N^2-1)}{6N} \left(\frac{c_{2,0}^{(j)}}{N} + c_{2,1}^{(j)} N \right), \\ c_3 &= \sum_j \frac{(N^2-1)}{3N} \left(\frac{c_{3,0}^{(j)}}{N^2} + c_{3,1}^{(j)} + c_{3,2}^{(j)} N^2 \right). \end{aligned} \quad (16)$$

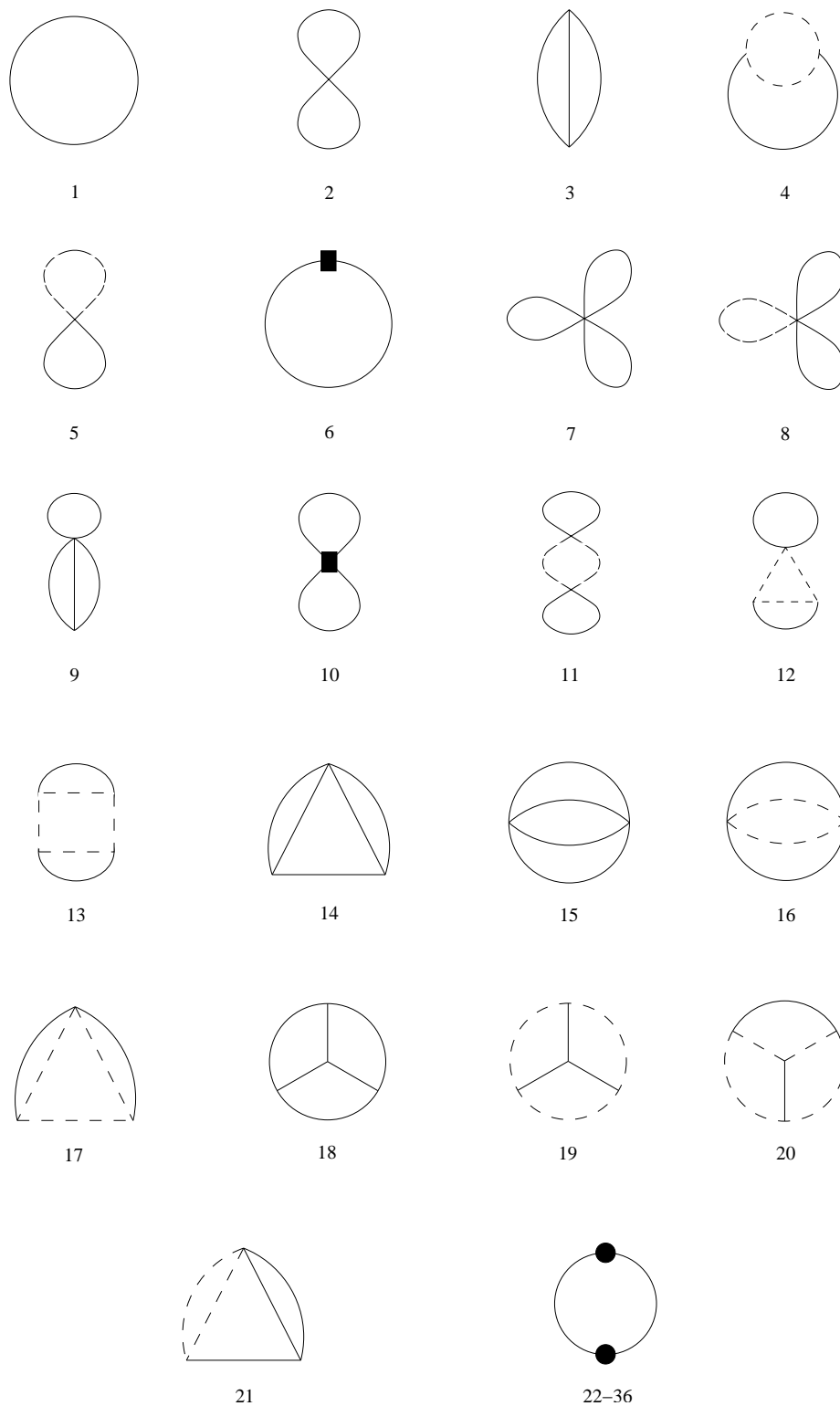


Fig. 1 Diagrams contributing to the Free Energy at one loop (1), two loops (2-6) and three loops (7-36). Solid (dashed) lines represent gluons (ghosts). The filled square is the contribution from the “measure” part of the action. Black bullets stand for an effective vertex, which is shown in Fig. 2.

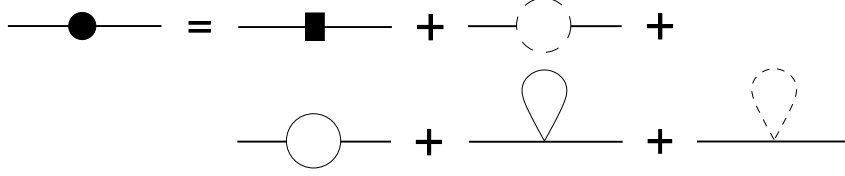


Fig. 2 Effective vertex involved in diagrams 22-36. The filled square is the contribution from the “measure” part of the action.

The index j runs over all contributing diagrams. The coefficients $c_{2,k}^{(j)}$, $c_{3,k}^{(j)}$ are pure numbers and we calculate them for each diagram separately. Their numerical values are listed in Tables I and II. For some diagrams, the coefficients are known analytically. The expressions are presented as a function of the 1-loop vacuum diagram P_1 (see below):

$$\begin{aligned}
c_{2,1}^{(2)} &= (1 + 28P_1 - 72P_1^2)/48 \\
c_{2,1}^{(5)} &= -P_1/12 \\
c_{2,1}^{(6)} &= -P_1/8 \\
c_{3,1}^{(7)} &= (504P_1 - 1296P_1^2 - 6)/5184 \\
c_{3,2}^{(7)} &= (3240P_1^3 - 792P_1^2 - 63P_1 - 1)/5184 \\
c_{3,2}^{(8)} &= -P_1^2/288 \\
c_{3,2}^{(10)} &= -P_1^2/384 \\
c_{3,2}^{(11)} &= -P_1^2/288
\end{aligned} \tag{17}$$

The value of P_1 can be expressed in terms of the Bessel function of the first kind I_0 :

$$\begin{aligned}
P_1 &= \int_{-\pi}^{\pi} \frac{d^3p}{(2\pi)^3} \frac{1}{4 \sum_{\mu=1}^3 \sin^2(p_{\mu}/2)} = \int_0^{\infty} dt \left[\int_{-\pi}^{\pi} \frac{dp}{(2\pi)} e^{-t} 4 \sin^2(p/2) \right]^3 = \int_0^{\infty} dt \left[e^{-2t} I_0(2t) \right]^3 \\
&= 0.2527310098590 \dots
\end{aligned} \tag{18}$$

The ghost loop in diagram 21 leads to a vanishing contribution by color antisymmetry.

Using our results we can express the average Free Energy as a function of g_0 , for specific values of N :

$$N = 2 : \quad \langle E \rangle = (1/4) g_0^2 + 0.01453916(1) g_0^4 + 0.0053459(2) g_0^6 + \dots \tag{19}$$

$$N = 3 : \quad \langle E \rangle = (4/9) g_0^2 + 0.05420318(2) g_0^4 + 0.0317648(7) g_0^6 + \dots \tag{20}$$

Presented in Fig. 3 is the behaviour of the average Free Energy as a function of $1/\beta$, for $N = 2$ and $N = 3$.

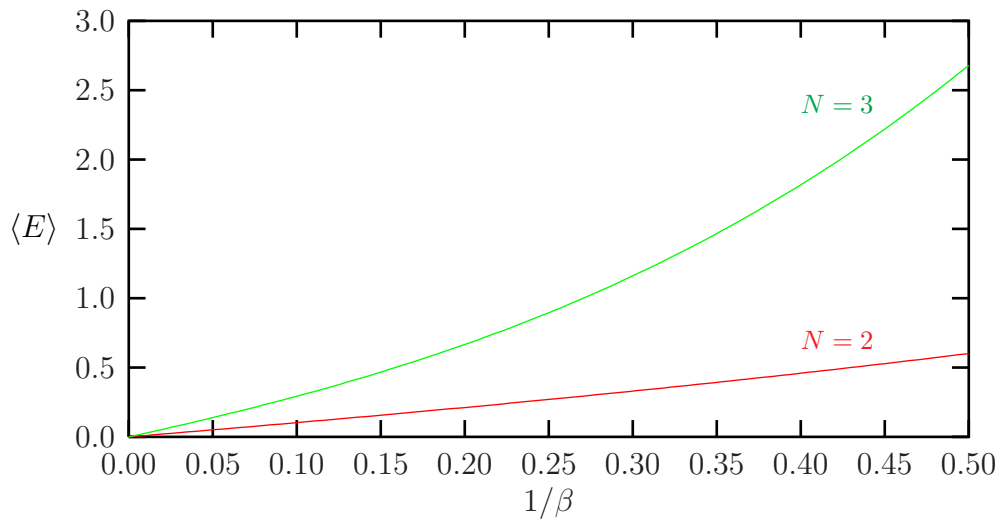


Fig 3 Average of Free Energy, as a function of $1/\beta$ for $N = 2$ and $N = 3$.
Systematic errors are too small to be visible.

IV. DISCUSSION AND CONCLUSIONS

Several remarks are in order regarding our computation.

- As mentioned above, certain subsets of diagrams are infrared finite when summed together, and they correspond to insertions of the one-loop renormalized gluon propagator. Similarly, diagrams 11, 12 and 13 renormalize the ghost propagator; however, they are separately finite.
- The manipulation of the algebraic expressions in order to reach a code for numerical loop integration, is completely done in Mathematica. The production of vertices as well as their contraction is fully automated. A number of routines render automatic the simplification of the expressions (such as color contractions and Lorentz index manipulation) and exploitation of their symmetries. We have also developed an efficient three dimensional “integrator” to automatically convert the integrand to Fortran code. The size of a typical input integrand is up to $\lesssim 1000$ terms after simplification. Finally, the extrapolation of data to infinite L is also automated. The only part which is done by hand is the enumeration of diagrams, but this is simple enough to do, even up to 4 loops. Each n -vertex diagram is represented by an $n \times n$ “incidence” matrix M , where M_{ij} is the number of gluons joining vertices i and j and by a similar matrix for ghosts. The procedure described above is not CPU intensive as regards symbolic manipulations in Mathematica. Of course, this is due to the usage of Wilson action for gluons (improved actions are more cumbersome in terms of CPU as well as RAM).
- Numerical integrals are performed for finite lattice sizes¹, up to $L = 100^3$, and the results are subsequently extrapolated to $L \rightarrow \infty$. Diagrams 18-20 (those having the form of the Mercedes emblem) are more CPU intensive and require approximately 40 hours each (for $L = 40^3$) on a recent PentiumIV computer (3.2 GHz); for these diagrams, integration over the three loop momenta can only be performed in a nested fashion, rather than in parallel. Fortunately, lattice sizes up to $L = 40^3$ already lead to a sufficiently small systematic error in these cases. For the rest of the diagrams, two out of the three loop momenta can be integrated in a parallel fashion, and the calculation requires approximately 1 hour per diagram for $L = 100^3$.

Extrapolation to infinite lattice size is of course a source of systematic error. To estimate this error, our procedure carries out the following steps: First, different extrapolations of our numerical data r_L are performed using a broad spectrum of functional forms $f^k(L)$ (around 50 of them) of the type:

$$f^k(L) = \sum_{i,j} e_{i,j}^{(k)} L^{-i} (\ln L)^j \tag{21}$$

A total of N_k coefficients appear in the k^{th} functional form; these coefficients are determined uniquely using the results on N_k lattices of consecutive size L .

¹A detailed treatment of the zero modes on a finite lattice is not necessary for the purposes of extrapolation to $L \rightarrow \infty$

For the k^{th} such extrapolation, a deviation d_k is calculated using alternative criteria for quality of fit. One possible criterion, as an example, is the difference: $d_k = |f^k(L^*) - r_{L^*}|$, where L^* is the largest lattice size which was not used in the determination of $e_{i,j}^{(k)}$. Finally, these deviations are used to assign weights $d_k^{-2}/(\sum_k d_k^{-2})$ to each extrapolation, producing a final value together with the error estimate. We can check the reliability of our error estimates in a number of ways: In those cases where the result for a diagram is also known analytically, this result coincides with the numerical one within the systematic error; also, extrapolations which incorporate new data from larger lattices are compatible with previous results, again within systematic error.

The 3-dimensional case is slightly different and more delicate than the case of 4 dimensions; in the latter only even powers of $1/L$ must be used ($i = \text{even}$ in Eq.(21)), along with possible logarithms. In 3 dimensions one must also use odd negative powers of L , since the main difference between a sum over discrete values of momenta and the corresponding integral comes from omitting the contribution of the zero mode. This quantity behaves like $I = \int_V d^3p/p^2$ where V is a sphere of diameter $2\pi/L$. We see that $I = 4\pi^2/L$.

Using larger lattices is of course computationally more feasible in 3 dimensions. At the same time, it is also more necessary than in 4-D, since the infrared behaviour of loop integrals worsens in 3-D. Suffice it to recall that 4-loop integrals in three dimensions will bring about a genuine divergence, requiring introduction of an IR regulator.

- Referring to diagrams 22-36, integration in 3-D with use of an IR regulator (in our case, L) may give extra terms which do not exist in the 4-D case, leading to potentially wrong results, when the regulator is taken to its limit value ($L \rightarrow \infty$). Due to the presence of a loop involving two propagators at the same momentum, each of these diagrams exhibits a behaviour of the type:

$$(a + \frac{b}{L})(cL + d) \quad (22)$$

After summing all diagrams and extrapolating to the limit $L \rightarrow \infty$, the result we get has the form $ad + bc$ (terms like acL add up to zero). Of course, the terms bc are spurious and must not be taken into account. A similar procedure in 4 dimensions leads instead to:

$$(a + \frac{b}{L^2})(c \ln L + d) \quad (23)$$

so that spurious terms are absent: $(b/L^2)(c \ln L) \rightarrow 0$. To solve this problem, we can write the mathematical expression for each vertex involved in diagrams 22-36 (Fig. 2) in a subtracted way: $f(p) = f(0) + (f(p) - f(0))$, where p is the momentum on external lines. Once all the subtracted vertices are summed, the terms $f(0)$ cancel among themselves. In addition to that, the terms $f(p) - f(0)$ are at least of first order in p and factors of the type cL involved in Eq. (22) cannot arise. The subtracted diagrams take the form $(\tilde{a} + \tilde{b}/L)(\tilde{d})$ and thus, extrapolation gives the desired results $\tilde{a}\tilde{d}$.

- For purposes of comparison, we can express the perturbative expansion of the Free Energy shown in Eqs. (19) and (20), as a function of $1/\beta$:

$$N = 2 : \quad \langle E \rangle = \left(\frac{1}{\beta}\right) + 0.2326265(2) \left(\frac{1}{\beta}\right)^2 + 0.34214(1) \left(\frac{1}{\beta}\right)^3 + \dots \quad (24)$$

$$N = 3 : \quad \langle E \rangle = (8/3) \left(\frac{1}{\beta}\right) + 1.951315(1) \left(\frac{1}{\beta}\right)^2 + 6.8612(2) \left(\frac{1}{\beta}\right)^3 + \dots \quad (25)$$

For the case $N = 3$, the value $(2N)^3 c_3 = 6.8612(2)$ improves a previous estimate $(2N)^3 c_3 = 6.90_{-0.12}^{+0.02}$ [8], which was obtained with the method of stochastic perturbation theory; it allows for a more stable extraction of the “finite” part of the gluon condensate, as expressed in Ref. [9] (using the notation of that reference for the symbols c_i):

$$8 \frac{(N^2 - 1) N^6}{(4\pi)^4} B_G = \lim_{\beta \rightarrow \infty} \beta^4 \left\{ \langle 1 - \frac{1}{N} \text{Tr}(P) \rangle - \left[\frac{c_1}{\beta} + \frac{c_2}{\beta^2} + \frac{c_3}{\beta^3} + \frac{c_4}{\beta^4} (\ln \beta + c'_4) \right] \right\} \quad (26)$$

where the logarithmic coefficient c_4 is known from the continuum vacuum energy density in the \overline{MS} scheme:

$$c_4 = 8 \frac{(N^2 - 1) N^6}{(4\pi)^4} \left(\frac{43}{12} - \frac{157}{768} \pi^2 \right), \quad c_4(N=3) = 2.92942132\dots \quad (27)$$

and c'_4 requires a 4-loop calculation in lattice perturbation theory.

- A possible extension of the present calculation to 4 loops is feasible with the techniques used in this paper, but one must take into account some additional difficulties: First of all there is a total of 250 diagrams to be calculated (43 pure gluon diagrams, 115 diagrams with one ghost loop, 37 diagrams with two ghost loops, 4 diagrams with three ghost loops and 51 diagrams with measure terms) and computation time is proportional to L^{12} (in most diagrams, loop integrals are factorizable, with the exception of a “nonplanar” diagram and its two ghost variants). Furthermore, due to the existence of a genuine logarithmic divergence, one must insert an IR cutoff m leading to results of the form $c \ln(m) + d$. Of course, the vertices and the contracted expressions, as well as a 4-loop version of our integrator, can still be produced automatically in this case.

Acknowledgements: This work is supported in part by the Research Promotion Foundation of Cyprus (Proposal Nr: ENTAE/0504/11).

TABLES

TABLE I. Per-diagram contributions to c_2 .

Diagram	$c_{2,0}$	$c_{2,1}$
2	-1/12	0.0724503107...
3	0	0.03394382(1)
4	0	-0.00383019(1)
5	0	-0.0210609174...
6	0	-0.0315913762...
Sum	-1/12	0.04991165(2)

TABLE II. Per-diagram contributions to c_3 .

Diagram	$c_{3,0}$	$c_{3,1}$	$c_{3,2}$
7	-1/216	0.00744542215...	-0.0029334803...
8	0	0	-0.0002217811...
9	0	0.01131461(2)	-0.01213765(2)
10	0	0	-0.0001663358...
11	0	0	-0.0002217811...
12	0	0	-0.00016133(1)
13	0	0	-0.00011990(1)
14	0	0	-0.00164058(1)
15	0.0094117909(2)	-0.00313726(1)	0.00306459(1)
16	0	0	-0.00011644(1)
17	0	0	-0.00008704(1)
18	0	0	0.00128600(6)
19	0	0	-0.00008896(2)
20	0	0	-0.00004025(1)
21	0	0	0
22-36	1/72	-0.03170827(1)	0.01911231(5)
Sum	0.0186710502(2)	-0.01608550(3)	0.00552737(9)

REFERENCES

- [1] A. Hietanen, K. Kajantie, M. Laine, K. Rummukainen and Y. Schröder, PoS (LAT2005) 174 [hep-lat/0509107].
- [2] E. Braaten, Phys. Rev. Lett. **74** (1995) 2164.
- [3] E. Braaten and A. Nieto, Phys. Rev. **D53** (1996) 3421 [hep-ph/9510408].
- [4] A. D. Linde, Rep. Prog. Phys. **42** (1979) 389; Phys. Lett. **B96** (1980) 289.
- [5] A. Di Giacomo and G. C. Rossi, Phys. Lett. **B100**, (1981) 481.
- [6] B. Allés, M. Campostrini, A. Feo and H. Panagopoulos, Phys. Lett. **B324** (1994) 433.
- [7] A. Athenodorou, H. Panagopoulos and A. Tsapalis, Nucl. Phys. **B140** (PS) (2005) 794 [hep-lat/0409127].
- [8] F. Di Renzo, A. Mantovi, V. Miccio and Y. Schröder, JHEP **05** (2004) 006 [hep-lat/0404003]; C. Torrero, F. Di Renzo, V. Miccio, M. Laine and Y. Schröder, PoS (LAT2005) 189 [hep-lat/0509157].
- [9] A. Hietanen, K. Kajantie, M. Laine, K. Rummukainen and Y. Schröder, JHEP **01** (2005) 013 [hep-lat/0412008].
- [10] H. Kawai, R. Nakayama and K. Seo, Nucl. Phys. **B189**, (1981) 40.